Delay in hepatocyte proliferation and prostaglandin D2 synthase expression for cholestasis due to endotoxin during partial hepatectomy in rats

（肝部分切除後ラットにおけるエンドトキシン誘発性胆汁うっ滞に伴う
肝再生遅延とプロスタグランジン D2 合成酵素発現）

申 請 者　　弘前大学大学院医学研究科
腫瘍制御学領域　消化器外科学分野

氏　　名　　若　狭　悠　介

指導教授　　袴　田　健　一

ABSTRACT

Background

Infection is a frequent complication of liver transplantation or partial hepatectomy (PH) and sometimes results in cholestasis. We examined factors involved in infection-induced cholestasis after PH, employing a rat PH model and lipopolysaccharide (LPS) as a bacterial toxin.

Methods

Male Sprague-Dawley rats were subjected to 70% PH and/or LPS injection, and tissues were harvested at 0, 24, 72, and 168 h. Gene expression was analyzed by microarray analysis and quantitative real-time polymerase chain reaction, and protein levels and localization were analyzed by western blotting and immunohistochemistry, respectively.

Results

Plasma bile acid levels were significantly higher in the LPS + PH group than in the PH group. Ribonucleotide reductase regulatory subunit M2 and proliferating cell nuclear antigen peaked at 24 and 72 h in the PH group and LPS + PH group, respectively, indicating a delay in cell proliferation in the latter group. The sodium-dependent taurocholate cotransporting polypeptide and organic-anion-transporting polypeptide 1a1 and 1a2 were reduced in the PH

group at 24 h, and were not further decreased in the LPS + PH group. Chemokine ligand 9 (Cxcl9), a chemokine involved in M2 macrophage polarization, increased after 24 h in the LPS and the LPS + PH groups. The number and shape of Cxcl9-positive cells were similar to CD163-positive cells, suggesting that such cells produced the chemokine. Hematopoietic prostaglandin D2 synthase (Ptgds2) was only detected in hepatocytes of the LPS + PH group exhibiting a delay in cell proliferation.

Conclusions

Thus, Kupffer cells activated with LPS were suggested to be responsible for a delay in hepatocyte proliferation after PH.

INTRODUCTION

The liver is a unique organ with a capacity to regenerate after removal of two-thirds of a liver mass [1]. Liver regeneration requires precisely coordinated proliferation of the two major hepatic cell populations, hepatocytes and liver sinusoidal endothelial cells to reconstitute liver structure and function [2]. Liver regeneration also requires the interaction between hepatocytes and other component cells such as Kupffer cells and hepatic stellate cells [1, 3, 4]. Many molecules such as hepatocyte growth factor and epidermal growth factor are demonstrated as mitogens to be produced in nonparenchymal cells [5]. Repressed liver regeneration is of major concern in a small remnant liver volume in adult living donor transplantation or in bacterial infection after partial hepatectomy, because this is associated with cholestasis and mortality [6].

Hepatocytes in physiological conditions efficiently extract bile acids from sinusoids by the sodium-dependent taurocholate cotransporting polypeptide (Ntcp) and the sodium-independent organic anion transporting polypeptide (Oatp1). The extracted bile acids are excreted into the bile canaliculi by ATP-dependent transporters, such as the bile salt export pump [7]. In our previous study, 90% partial hepatectomy in rats resulted in the high blood

bile acids levels and repression of Ntcp expression. Thus, lower uptake of bile acids is suggested to be partly involved in cholestasis [6].

Infection is a frequent complication after living donor liver transplantation [8].

Low-dose lipopolysaccharide (LPS) application after PH in mice is reported to cause a delay of liver proliferation [9]. Because LPS is known to activate Kupffer cells [10], this finding suggests that activated Kupffer cells may repress liver proliferation. However, many studies have demonstrated that Kupffer cells stimulate liver regeneration after PH [1] and depletion of Kupffer cells by clodronate delays the regeneration [11]. Therefore, Kupffer cells activated with LPS seem to lose the capacity to proliferate hepatocytes after PH.

In the present study, we found that LPS treatment induced cholestasis and delayed cell proliferation in the rat 70% PH model. Expression of anion transporters for the uptake from the sinusoid was decreased in PH but LPS did not further decrease their expression. This suggested that decreases in these transporters were not responsible, but a delay in hepatocyte proliferation was responsible for LPS-induced cholestasis. LPS treatment alone or in combination with PH induced Kupffer cell activation with a

CD163-positive phenotype, a marker for M2-type macrophages [12] and CD163-positive cells were suggested to produce Cxcl9, a chemokine involved in chronic inflammation [13] and M2 macrophage polarization [14]. Because hematopoietic type prostaglandin D2 synthetase (Ptgds2) was known to inhibit lymphocyte proliferation [15], Ptgds2 staining was performed. Hepatocytes in the LPS + PH group were stained and markedly stained at 24 h, a time point when cell proliferation was highly inhibited. On the other hand, hepatocytes in the LPS or the PH groups were not stained.

MATERIALS AND METHODS

Animals and animal treatment

Male Sprague-Dawley rats weighing 180-220 g and 6 weeks old were purchased from Charles River Laboratories Japan, Inc. (Tsukuba, Japan). They were kept under routine laboratory conditions at the animal laboratory of Hirosaki University. The rats received standard laboratory chow, had free access to food and water, and were kept in a thermostatically controlled room (25 ° C) with a 12-h light-dark cycle. Before undergoing surgical procedures, all rats were fasted for 24 h. The rats were divided into five groups: control group without any treatment, sham group receiving laparotomy alone, LPS group receiving intravenous LPS 75 μg/rat, PH group receiving 70% PH, and LPS + PH group receiving intravenous LPS injection immediately after PH. 70% PH was performed as reported previously [6]. The rats of four groups except the control group were sacrificed at 24 h, 72 h, and 168 h after laparotomy or PH and/or LPS treatment. Those of the control group were sacrificed at 0 h. Three rats each were used at respective time points of each group. LPS (055:B5, L2880) was purchased from Sigma-Aldrich (Tokyo, Japan). After the surgical procedures, the rats had free access to a 200 g/L glucose solution for 24 h to avoid post-operative hypoglycemia after hepatectomy. This study was

performed in accordance with the Guidelines for Animal Experimentation, Hirosaki University, and all of the animals received humane care according to the criteria outlined in the ‘Guide for the care and use of laboratory animals’ prepared by the National Academy of Sciences and published by the National Institutes of Health (NIH publication 86-23, revised 1985).

Plasma total bilirubin and bile acids

Plasma total bilirubin, aspartate aminotransferase (AST), and alanine aminotransferase (ALT) were measured using Spotchem EZ (ARKRAY, Inc., Minneapolis, MN, USA) with SPOTCHEM II Basic Panel 2 Test Strips (MT-7785). Plasma total bile acids level was measured with an assay kit (Diazyme Laboratories, Poway, CA, USA).

Microarray analysis

Total RNA was extracted from frozen liver samples at 0, 24, 72, and 168 h after 70% hepatectomy and/or LPS injection with TRIzol reagent (Invitrogen, Carlsbad, CA). Equal amounts of RNA from three individual livers were combined, and 10 μg of RNA was used for biotin-labeled complementary RNA (cRNA). The labeled and fragmented cRNA was subsequently hybridized to GeneChip® Rat Gene-

ST 2.0 Array (Affymetrix, Santa Clara, CA). Labeling, hybridization, image scanning, and data analysis were performed at TOHOKU CHEMICAL Co., Ltd. (Iwate, Japan).

Quantitative real-time polymerase chain reaction (RT-PCR)

Complementary DNA (cDNA) was reverse-transcribed from 1 μg of total RNA using the Omniscript RT kit (Qiagen, Tokyo, Japan). A MiniOpticon Detection System (Bio-Rad Laboratories, Hercules, CA) and SYBR Green Supermix (Bio-Rad Laboratories) were used for the quantitation of specific messenger RNA (mRNA). The amplification of *ubiquitin C* cDNA was performed to standardize the levels of the target cDNA, as reported previously [6]. Gene-specific primers were designed according to known rat sequences (**Table 1**). No non-specific PCR products, as detected by melting temperature curves, were found. After normalizing the expression of the target gene to *ubiquitin C* expression using the $2^{-\Delta\Delta CT}$ method of Livak and Schmittgen [16] with triplicate assay, the levels of expressed mRNA in 3 samples at respective time points were expressed relative to the control values.

Western blotting

Crude liver membranes were prepared according to the method of Gant et al [17] and preparations (100 μg protein each) were dissolved in sample buffer and loaded onto a 7.5% sodium dodecyl sulfate polyacrylamide electrophoresis gel with a 4.4% stacking gel. After electrophoresis, the proteins were transferred to polyvinylidene fluoride membranes (Hybond-P, GE Healthcare, Buckinghamshire, UK). After blocking, membranes were incubated overnight at 4 °C with primary anti-Ntcp antibody (sc-107029) (1:10,000, Santa Cruz Biotechnology, Inc., Santa Cruz, CA) or anti-β-actin antibody (ab227387)(1:1,000, Abcam, Tokyo, Japan). Immune complexes were detected using a horseradish peroxidase conjugated anti-rabbit IgG secondary antibody and an enhanced chemiluminescent kit (ECL Plus; GE Healthcare).

Immunostaining

Liver tissue samples were fixed in 10% neutral buffered formaldehyde and embedded in paraffin. These paraffin blocks were stained for HE, CD68, CD163, chemokine (C-X-C motif) ligand 9 (Cxc19), and hematopoietic prostaglandin D2 synthase (Ptgds2). Immunohistochemical staining was performed on deparaffinized sections using a standard avidin-biotin-peroxidase conjugate method using an automated immunostaining instrument (Benchmark XT; Ventana

Medical System, Tucson, AZ, USA). Primary antibodies were anti-CD68 antibody of AbD serotype (MCA 341 R) (Oxford, UK), anti-CD 163 antibody (sc-58965) (Santa Cruz Biotechnology, Inc., Santa Cruz, CA), anti-Cxcl9 antibody (Bioss, Boston, MA), and anti-Ptgds2 antibody (PA 5-43217) (Invitrogen, Waltham, MA). Non-immune γ-globulin was used as a negative control instead of primary antibody. Images were captured with an Olympus FSX 100 microscope (Olympus, Tokyo, Japan). Digital images were processed with Adobe Photoshop (Adobe, San Jose, CA) and ImageJ software (Wayne Rasband NIH, Bethesda, MD).

Statistical analysis

Data are presented as mean ± SD. Differences between experimental groups were assessed for significance using the two-way ANOVA with Tukey's test. P values <0.05 were considered significant.

RESULTS

Elevated plasma bilirubin and bile acid levels in the LPS + PH group

Bilirubin and bile acid levels in plasma at 24 h post-operation were increased in the LPS + PH group, compared with those in the sham group. The bile acid level was significantly higher in the LPS + PH group than that in the PH group (**Fig. 1**). These results indicated that LPS induced cholestasis in this rat model. AST and ALT levels in plasma at 24 h were increased in the LPS + PH group and PH group, compared with those in the sham group.

Suppression and delay in DNA replication in the LPS + PH group

Microarray was performed to comprehensively analyze alterations in liver gene expression. Data were expressed as signal values, and changes of more than 2-fold or less than 1/2 from the values in the control or sham groups were considered significant. Ribonucleotide reductase regulatory subunit M2 (*Rrm2*), DNA topoisomerase II alpha (*Top2a*), and proliferating cell nuclear antigen (*Pcna*), which are markers of DNA replication, reached a peak level of expression after 24 h in the PH group and gradually decreased thereafter. However, in the LPS + PH group, these replication signals were low after 24 h and peaked after 72 h. The values at 72 h were less than those at 24 h in the PH group. These results revealed a delay and suppression in DNA replication

in the LPS + PH group. No changes were observed in *Cd68* or *Cd163* expression, which are markers of Kupffer cells. The chemokine *Cxc19* markedly increased in the LPS group and LPS +PH group, compared with that in the sham at 24 h (**Table 2**). For sinusoid transporters, sodium-dependent taurocholate cotransporting polypeptide (Ntcp, gene symbol *Slc10a1*), solute carrier organic anion transporters 1a1 (Oatp1, gene *Slc21a1*) and 1a2 (Oatp2, gene *Slc21a2*) were reduced in the LPS + PH group and the PH group at 24 h. These expression levels returned to control levels at 72 h in both groups. No changes were observed in collagen 1α1 (*Col1a1*) or desmin (*Des*), markers of hepatic stellate cells, or in cytokeratin19 (*Krt19*) or epithelial cell adhesion molecule (*Epcam*), markers of liver progenitor cells.

To confirm these changes in gene expression, RT-PCR was performed. ATP binding cassette subfamily C member 2 (Mrp2, gene *Abcc2*), Oatp1, and Oatp2 mRNA levels were significantly decreased at 24 h in the LPS + PH group and PH group, compared with those in the sham group. These mRNA levels except Oatp2 were not significantly different between the LPS + PH group and the PH group (**Fig. 2a**). The Rrm2 mRNA level at 24 h in the LPS + PH group was lower than the value in the PH group (**Fig. 2b**). Rrm2 and Pcna peaked at 24 h in the PH group whereas at 72 h in the LPS + PH group (**Fig. 2b**), confirming the results

obtained by microarray analysis. *Cxcl9* showed a marked rise after 24 h in the LPS group and LPS + PH group (**Fig. 2b**). This finding suggested that *Cxcl9* expression was dependent on LPS treatment.

Ntcp protein levels were examined by western blotting, and Ntcp was decreased in the PH group and LPS + PH group at 24 h (**Fig. 3**).

Expression of Cxcl9 in Kupffer cells activated by LPS treatment

Although *Cd68* mRNA or *Cd163* mRNA levels were not altered by microarray analysis (**Table 2**), staining for CD68, a marker for Kupffer cells and macrophages, revealed a marked increase in CD68-positive Kupffer cells in the LPS group and LPS + PH group, compared with that in the sham and PH groups (**Fig. 4a**). CD 163 staining, a marker for M2 macrophages and Kupffer cells [12], was positive in cells in the LPS group and LPS + PH group (**Fig. 4b**). These CD163-positive cells were not detected in the sham or PH groups. There were fewer CD163-positive cells than CD68-positive cells, and their cell shapes were different from each other. These results suggested that CD163-positive cells detected after LPS treatment denoted M2-type Kupffer cells [12]. There were Cxcl9-positive cells in the LPS group and LPS + PH group (**Fig. 4c**), whereas Cxcl9-positive cells were not detected in the sham or PH groups. The number

and cell shape of Cxcl9-positive cells were similar to those of CD163-positive cells rather than CD68-positive cells (**Fig. 4d**).

Expression of Ptgds2 in hepatocytes in the LPS + PH group

Because Ptgds2 inhibits cell proliferation [15], Ptgds2 staining was performed. A positive reaction was only detected in hepatocytes in the LPS + PH group and not in other groups (**Fig. 5**). Kupffer cells were not stained in any groups. In the LPS + PH group, Ptgds2 was markedly stained in hepatocytes at 24 h, weakly stained at 72 h, and not at all at 168 h.

DISCUSSION

In this rat PH model, LPS treatment induced cholestasis (**Fig. 1**) and delayed cell proliferation (**Table 2 and Fig. 2b**). The expression of anion transporters involved in the uptake from the sinusoid was downregulated at 24 h in both the PH group and the LPS + PH group, but was not different between them (**Fig. 2b and Fig. 3**). Downregulation of these anion transporters is a causative factor for cholestasis after 90% PH [6, 7, 18]. However, this was unlikely in the case of cholestasis in the LPS + PH group. Suppression or delay in cell proliferation may be the responsible factor. Downregulation of marker genes of DNA replication such as *Rrm2* was supported by RT-PCR analysis. However, delay in cell proliferation is not confirmed by protein levels, because immunohistochemistry for PCNA is not successful yet. Hepatocyte proliferation is blocked by 2-acetylaminofluorene administration during partial hepatectomy in rats [19]. In this case, biliary epithelial cells and hepatic stellate cells become progenitor cells, and these cells contribute to liver regeneration. In the case of LPS, activation of these cells was not detected (**Table 2**), and hepatocyte proliferation was inhibited transiently.

LPS treatment increased CD68-positive cells and CD163-positive cells (**Fig. 4a, 4b, and 4d**). These results confirmed the activation of Kupffer

cells by LPS reported by other investigators [20]. In a microarray analysis, *Cd68* or *Cd163* expression was not altered by LPS treatment despite increased CD68-positive or CD163-positive cells by immunostaining. This discrepancy may reflect a difference between mRNA and protein, but the exact reasons remain unclear. Because CD163 is a marker for M2-type macrophages [12, 21], CD163-positive cells may belong to M2-Kupffer cells [21]. Thus, CD68-positive cells may denote M1-type macrophages or Kupffer cells [22]. A marked increase in CD68-positive cells by LPS treatment raises two possibilities: the proliferation of CD68-positive cells in the liver or the migration of CD68-positive cells to the liver from bone marrow [23, 24]. The absence of alteration in Cd68 mRNA levels by LPS treatment suggests the latter explanation as a more likely possibility.

In this experiment, *Cxcl9* was strongly induced by LPS treatment (**Table 2, Figs. 2b and 4c**). Immunohistochemistry suggested that Cxcl9 was produced in CD163-positive cells. Double staining for Cxcl9 and CD163 on the single slide will be necessary to establish this possibility. Cxcl9 is a member of a family of ligands for the Cxcr3 receptor, which is involved in chronic inflammation and cancer [13]. Cxcl9 is also a biomarker of acute cellular rejection after liver transplantation [25]. Endothelial cell growth is

stimulated or inhibited depending on alternatively spliced variants of Cxcr3 [26]. Cxcl9 is expressed in macrophages [27, 28], and CXCR3 promotes M2 macrophage polarization in human liver cancer [14]. Prostaglandin E2 inhibits CXCR3 ligand secretion induced by interferon-γ treatment in human breast cancer cells [29].

Ptgds2 is the hematopoietic-type Ptgds and is expressed in mast cells and macrophages [30]. Ptgds2 is also expressed in skeletal muscle cells with muscular dystrophy [31]. Inhibition of Ptgds2 stimulates the survival of muscle cells by suppression of muscular cell death [32]. Lymphocytes isolated from Ptgds2 knock-out mice exhibit hyperproliferation [15]. The time courses of Ptgds2 staining and cell proliferation had opposite profiles (**Fig. 5, Fig. 2b and Table 2**). Thus, Ptgds2 was suggested to suppress hepatocyte proliferation. Ptgds2 was not expressed in the LPS group or PH group, but was expressed in hepatocytes in the LPS + PH group. These results indicated that both LPS and cell proliferation signals were required for Ptgds2 expression in hepatocytes. The finding that LPS alone did not alter cell proliferation suggested that a delay in cell proliferation in the LPS + PH group was not because of the direct effects of LPS on hepatocytes, but because of Kupffer cells activated by LPS. Cxcl9 may be a candidate signaling molecule released

from Kupffer cells for Ptgds2 expression in hepatocytes. However, because Cxcl9 was produced by LPS alone, Cxcl9 is not sufficient for Ptgds2 expression. Ptgds2 may be a target to prevent a delay in cell proliferation after PH induced by LPS or bacterial infection.

ACKNOWLEDGEMENT

The authors thank Ms. Yukie Fujita and Sayumi Kubo (Department of Pathology and Bioscience, Hirosaki University Graduate School of Medicine) for their technical assistance in immunostaining, and Ms. Ryoko Seito, Mr. Hitoshi Kudo, and Ms. Ikumi Shirahama (Institute for Animal Experimentation, Hirosaki University Graduate School of Medicine) for their technical assistance for animal treatment.

CONFLICT OF INTEREST

None declared.

REFERENCES

1. Preziosi ME, Monga SP: Update on the mechanisms of liver regeneration. Semin Liver Dis. 2017; 37: 141-51.

2. Hu J, Srivastava K, Wieland M, et al: Endothelial cell-derived angiopoietin-2 controls liver regeneration as a spatiotemporal rheostat. Science. 2014; 343: 141-51.

3. Marrone G, Shah VH, Bracia-Sancho J: Sinusoidal communication in liver fibrosis and regeneration. J Hepatol. 2016; 65: 608-17.

4. Mabuchi A, Mullaney I, Sheard PW, et al: Role of hepatic stellate cell/hepatocyte interaction and activation of hepatic stellate cells in the early phase of liver regeneration in the rat. J Hepatol. 2004; 40: 910-16.

5. DeLeve LD: Liver sinusoidal endothelial cells and liver regeneration. J Clin Invest. 2013; 123: 1861-66.

6. Miura T, Kimura N, Yamada T, et al: Sustained suppression and translocation of Ntcp and expression of Mrp4 for cholestasis after rat 90% partial hepatectomy. J Hepatol. 2011; 55: 407-14.

7. Cuperus FJ, Claudel T, Gautherot J, et al: The role of canalicular ABC transporters in cholestasis. Drug Metab Dispos. 2014; 42: 546-60.

8. Abad CL, Lahr BD, Razonable RR: Epidemiology and risk factors for infection after living donor liver transplantation. Liver Transpl. 2017: 23: 465-77.

9. Jorger AK, Liu L, Fehlner K, et al: Impact of NKT cells and LFA-1 on liver regeneration under subseptic conditions. PLoS One. 2016; 11: e0168001.

10. Liu H, Liao R, He K, et al: The SMAC mimetic birinapant attenuates lipopolysaccharide-induced liver injury by inhibiting the tumor necrosis factor receptor-associated factor 3 degradation in Kupffer cells. Immunol Lett. 2017; 185: 79-83.

11. Meijer C, Wiezer MJ, Diehl AM, et al: Kupffer cell depletion by Cl2MDP-liposomes alters hepatic cytokine expression and delays liver regeneration after partial hepatectomy. Liver. 2000; 20: 66-77.

12. Edin S, Wikberg ML, Dahlin AM, et al: The distribution of macrophages with a M1 or M2 phenotype in relation to prognosis and the molecular characteristics of colorectal cancer. PLoS One. 2012; 7: e47045.

13. Billottet C, Quemener C, Bikfalvi A: CXCR3, a double-edged sword in tumor progression and angiogenesis. Biochim Biophys Acta. 2013; 1836: 287-95.

14. Liu RX, Wei Y, Zeng QH, et al: Chemokine (C-X-C motif) receptor 3-positive B cells link interleukin-17 inflammation to protumorigenic macrophage polarization in human hepatocellular carcinoma. Hepatology. 2015; 62: 1779-90.

15. Trivedi SG, Newson J, Rajakariar R, et al: Essential role for hematopoietic prostaglandin D2 synthase in the control of delayed type hypersensitivity. Proc Natl Acad Sci U S A. 2006; 103: 5179-84.

16. Livak KJ, Schmittgen TD: Analysis of relative gene expression data using real-time quantitative PCR and the 2 $^{-\Delta\Delta CT}$ method. Methods. 2001; 25: 402-8.

17. Gant TW, Silverman JA, Bisgaard HC, et al: Regulation of 2-acetylaminofluorene- and 3-methylcholanthrene-mediated induction of multidrug resistance and cytochrome P450IA gene family expression in primary hepatocyte cultures and rat liver. Mol Carcinog. 1991; 4: 499-509.

18. Chang TH, Hakamada K, Toyoki Y, et al: Expression of MRP2 and MRP3 during liver regeneration after 90% partial hepatectomy in rats. Transplantation. 2004; 77: 22-7.

19. Kordes C, Sawitza I, Götze S, et al: Hepatic stellate cells contribute to progenitor cells and liver regeneration. J Clin Invest. 2014; 124: 5503-15.

20. Suzuki S, Nakamura S, Serizawa A, et al: Role of Kupffer cells and the spleen in modulation of endotoxin-induced liver injury after partial hepatectomy. Hepatology. 1996; 24: 219-25.

21. Dixon LJ, Barnes M, Tang H, et al: Kupffer cells in the liver. Compr Physiol. 2013; 3: 785-97.

22. Tacke F, Zimmermann HW: Macrophage heterogeneity in liver injury and fibrosis. J Hepatol. 2014; 60: 1090-6.

23. Aldeguer X, Debonera F, Shaked A, et al: Interleukin-6 from intrahepatic cells of bone marrow origin is required for normal murine liver regeneration. Hepatology. 2002; 35: 40-8.

24. Nishiyama K, Nakashima H, Ikarashi M, et al: Mouse CD11b+Kupffer cells recruited from bone marrow accelerate liver regeneration after partial hepatectomy. PLoS One. 2015; 10: e0136774.

25. Asaoka T, Marubashi S, Kobayashi S, et al: Intragraft transcriptome level of CXCL9 as biomarker of acute cellular rejection after liver transplantation. J Surg Res. 2012; 178: 1003-14.

26. Lasagni L, Francalanci M, Annunziato F, et al: An alternatively spliced variant of CXCR3 mediates the inhibition of endothelial cell growth induced by IP-10, Mig, and I-TAC, and acts as functional receptor for platelet factor 4. J Exp Med. 2003; 197: 1537-49.

27. Farber JM: A macrophage mRNA selectively induced by gamma-interferon encodes a member of the platelet factor 4 family of cytokines. Proc Natl Acad Sci U S A. 1990; 87: 5238-42.

28. Metzemaekers M, Vanheule V, Janssens R, et al: Overview of the mechanisms that may contribute to the non-redundant activities of interferon-inducible CXC chemokine receptor 3 ligands. Front Immunol. 2017; 8: 1970.

29. Bronger H, Kraeft S, Schwarz-Boeger U, et al: Modulation of CXCR3 ligand secretion by prostaglandin E2 and cyclooxygenase inhibitors in human breast cancer. Breast Cancer Res. 2012; 14: R30.

30. Gandhi UH, Kaushal N, Ravindra KC, et al: Selenoprotein-dependent up-regulation of hematopoietic prostaglandin D2 synthase in macrophages is mediated through the activation of peroxisome proliferator-activated receptor (PPAR) gamma. J Biol Chem. 2011; 286: 27471-82.

31. Okinaga T, Mohri I, Fujimura H, et al: Induction of hematopoietic prostaglandin D synthase in hyalinated necrotic muscle fibers: its implication in grouped necrosis. Acta Neuropathol. 2002; 104: 377-84.

32. Mohri I, Aritake K, Taniguchi H, et al: Inhibition of prostaglandin D synthase suppresses muscular necrosis. Am J Pathol. 2009; 174: 1735-44.

FIGURE LEGENDS

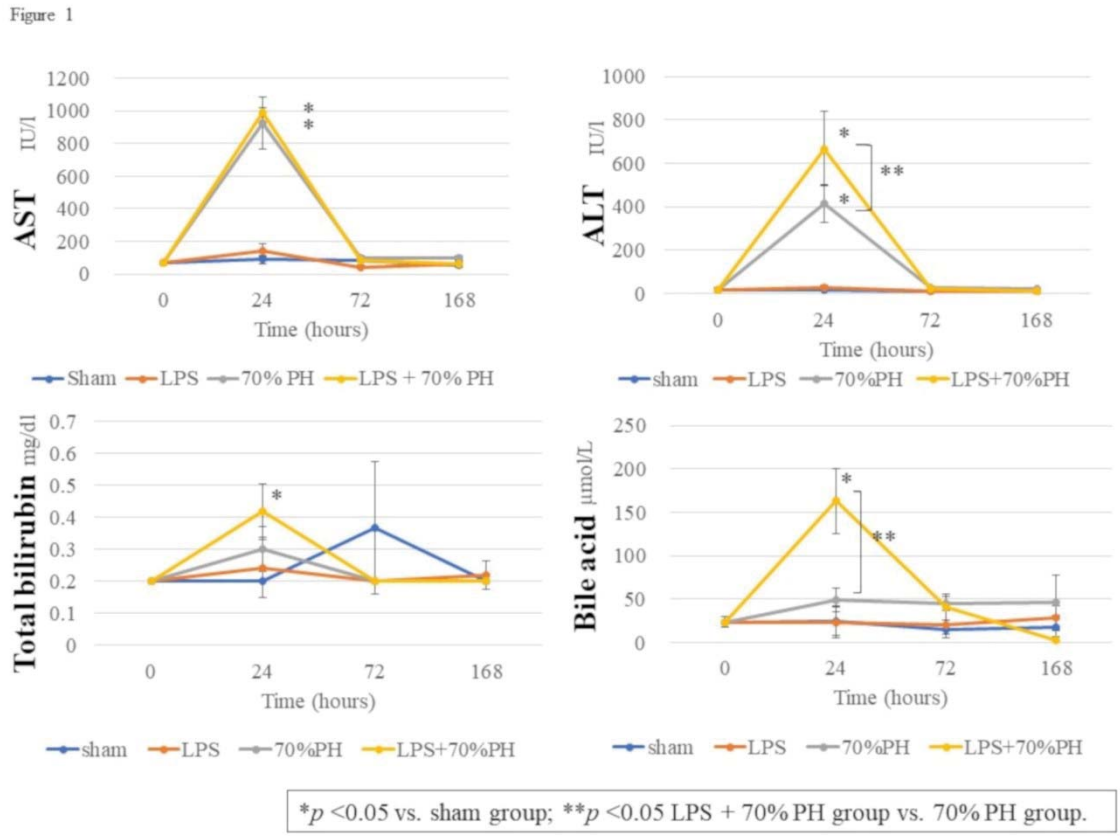

Fig. 1. Levels of plasma aspartate aminotransferase (AST), alanine aminotransferase (ALT), total bilirubin (T-Bil), and bile acids at 0 h (control), and 24, 72, and 168 h after a sham operation (blue), LPS administration (orange), 70% partial hepatectomy (PH) (gray), and LPS + 70% PH (yellow). The biomarker levels were quantified with a commercial kit. Data are the mean ± SD from three rats. *p <0.05 vs. sham group; **p <0.05 LPS + 70% PH group vs. 70% PH group.

Figure 2a

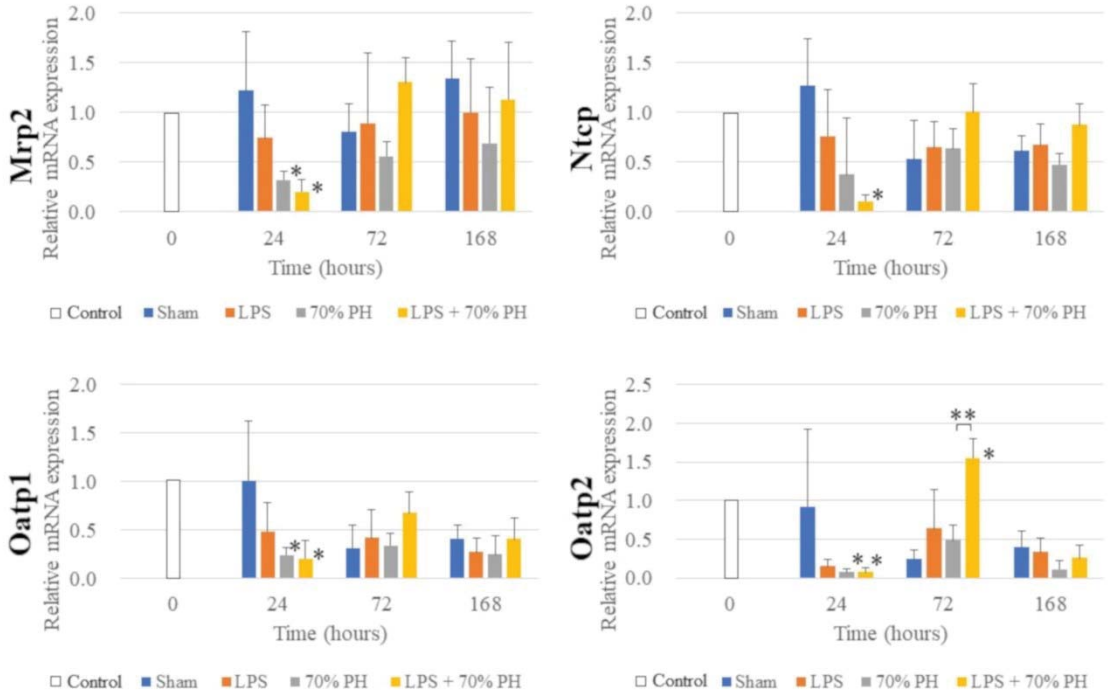

*p <0.05 vs. sham group; **p <0.05 LPS + 70% PH group vs. 70% PH group.

Figure 2b

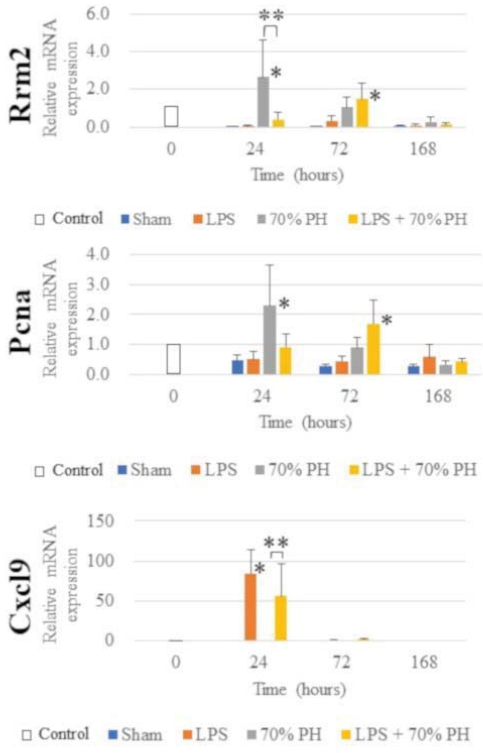

*p <0.05 vs. sham group; **p <0.05 LPS + 70% PH group vs. 70% PH group.

Fig. 2. The quantitation of mRNA for organic anion transporters (**a**), DNA replication genes, and Cxcl9 (**b**) at 0 h (control, white bar), and 24, 72, and 168 h after a sham operation (blue), LPS administration (orange), PH (gray), and LPS + PH (yellow). The quantification of Mrp2, Ntcp, Oatp1, Oatp2, Rrm2, Pcna, and Cxcl9 mRNA by RT-PCR is described in the Materials and methods and **Table 1**. The levels of mRNA at 24, 72, and 168 h are expressed relative to the values of individual mRNA at 0 h. Data are the mean ± SD from three rats. *$p < 0.05$ vs. sham group; **$p < 0.05$ LPS + PH group vs. PH group.

Figure 3

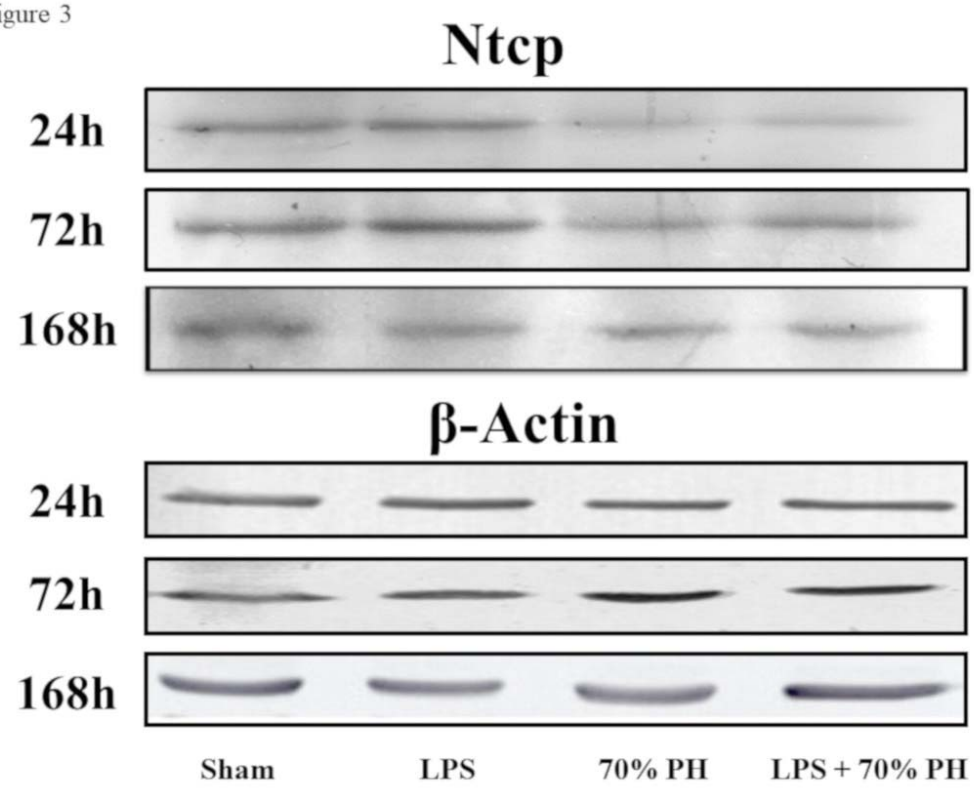

Fig. 3. Western blotting results for Ntcp in liver tissue membrane fractions at 24, 72, and 168 h after each operation and for β-actin at 24, 72, and 168 h for the loading control. Each lane contains 100 μg of protein.

Figure 4a

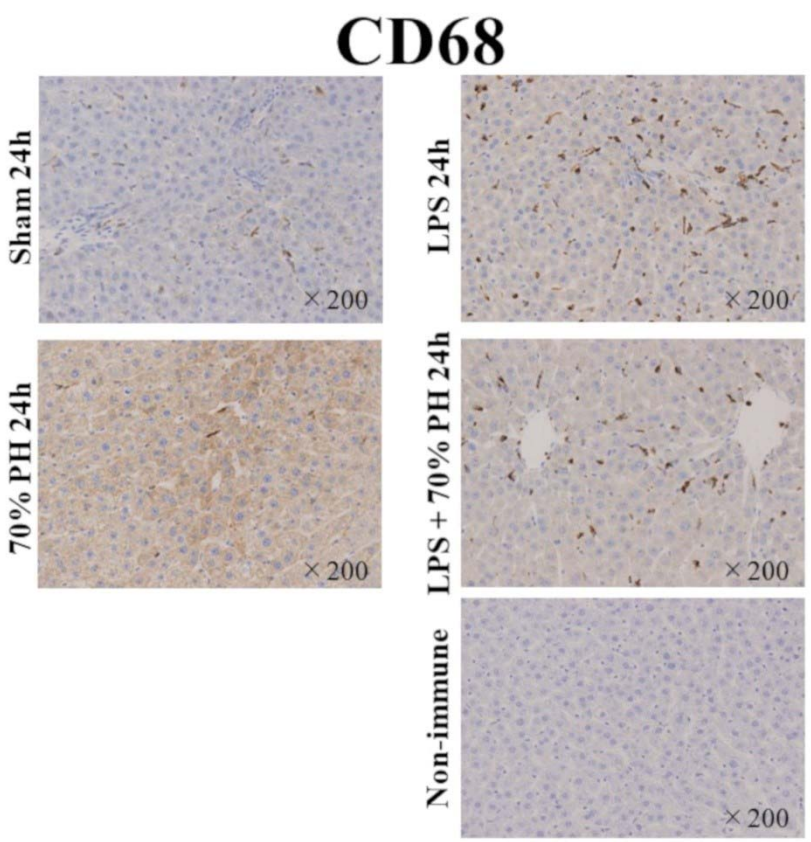

Figure 4b

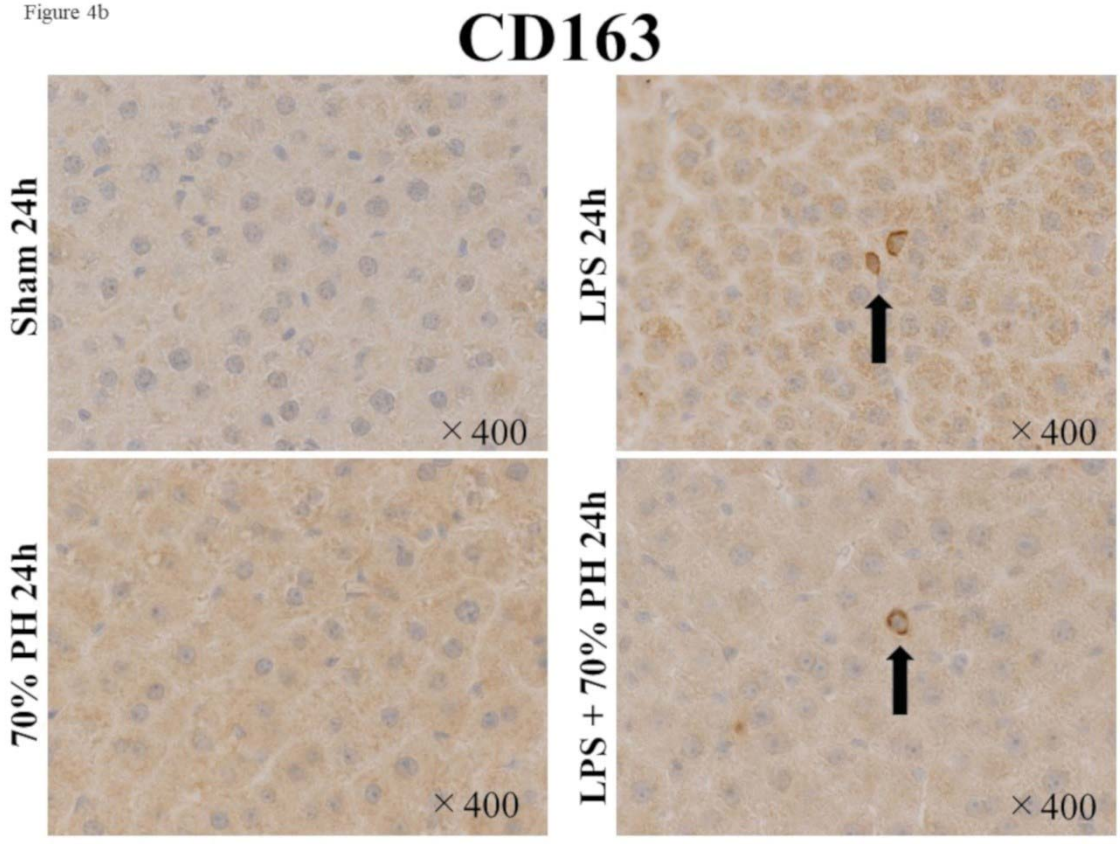

Figure 4c

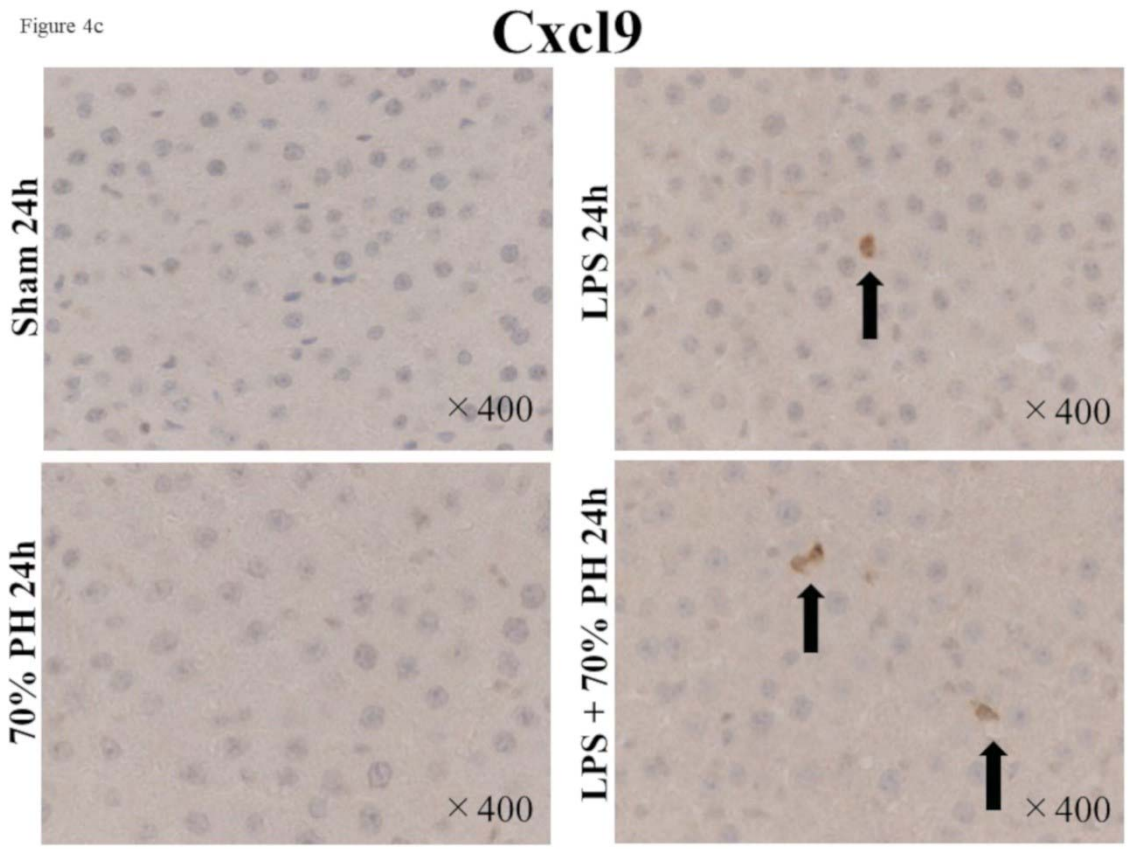

Figure 4d

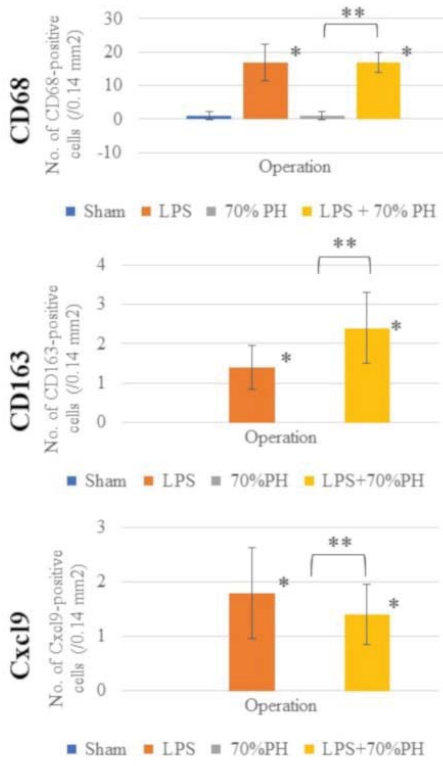

*p <0.05 vs. sham group; **p <0.05 LPS + 70% PH group vs. 70% PH group.

Fig. 4. Immunostaining for CD68 (**a**), CD163 (**b**), and Cxcl9 (**c**) in the sham group, LPS administration group, PH group, and LPS +PH group on 24 h. Staining result with non-immune γ-globulin is added to (**a**). Arrows in the panels show positive cells. The data shown are from a representative preparation set and are similar to results obtained in other sets. Original magnification: (**a**) 200× and (**b, c**) 400×. (**d**) Number of CD68-, CD163-, and Cxcl9-positive cells. The cells in the liver sections were from five microscope fields (0.14 mm2) for each rat. Data are the mean ± SD from three rats. *p <0.05 vs. sham group; **p <0.05 LPS + PH group vs. PH group.

Figure 5

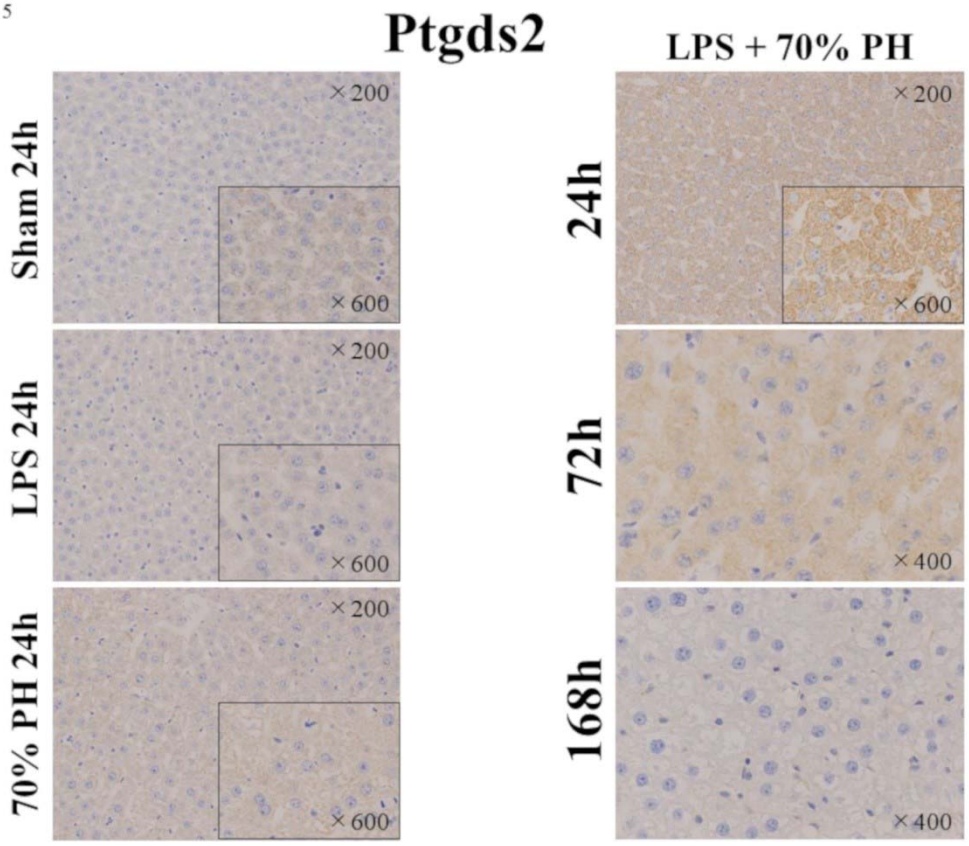

Fig. 5. Immunostaining for hematopoietic prostaglandin D2 synthase (Ptgds2) in the sham group, LPS administration group, PH group, and LPS + PH group at 24 h. Original magnification: 200×, and the small panels are a higher magnification (600×) of the original panel. Immunostaining for Ptgds2 in LPS + PH group on 72, and 168 h (original magnification: 400×).

Table 1. RT-PCR primer sequences.

Gene	5'-Primer (5'-3')	3'-Primer (5'-3')
Abcc2	CACAGGTTTGCCCATTATCC	ATATTGAGGGCGTTGGACAG
Slc10a1	AGGCATGATCATCACCTTCC	AAGTGGCCCAATGACTTCAG
Slco1a1	TACATGTCAGCTTGCCTTGC	GCGGGAATACCAGCAAATAC
Slco1a2	CAATTCGGTATCCCCACATC	GTTTGAGGACACGTTGCTTG
Rrm2	GCACTGGGAAGCTCTGAAAC	GGCAATTTGGAAGCCATAGA
Pcna	GGTGAAGTTTTCTGCGAGTG	CTCAGAAGCGATCGTCAAAG
Cxcl9	TCGAGGAACCCTAGTGATAAGGAATCAG	TTTGCTTTTTCTTTTGGCTGATCTTTTTC

Table 2. The results of microarray analysis.

Cellular function and gene name (*gene symbol*)	Signal												
		Sham			LPS			70% PH			LPS + 70% PH		
	control (0 h)	24 h	72 h	168h	24 h	72 h	168h	24 h	72 h	168h	24 h	72 h	168h
DNA replication													
ribonucleotide reductase subunit M2 (*Rrm2*)	450	40	30	70	70	420	120	2290*	660	270	470	860	40
topoisomerase(DNA) II alpha (*Top2a*)	250	30	40	70	70	190	70	750*	260	120	190	390	30
proliferating cell nuclear antigen (*Pcna*)	240	120	160	130	170	200	130	540*	250	170	240	300	190
DNA ligase I (*Lig1*)	60	30	40	60	50	70	60	120*	80	50	60	110	40
Kupffer cells													
Cd68 molecule (*Cd68*)	240	280	240	260	260	230	210	170	300	360	260	300	450
Cd163 molecule (*Cd163*)	260	320	250	260	200	270	250	230	310	350	270	300	380
mannose receptor, C type 1 (*Mrc1*)	450	550	440	490	420	580	490	400	510	520	370	570	570
chemokine (C-X-C motif) ligand 1 (*Cxcl1*)	50	110	120	70	120	50	60	470*	250*	230*	260*	210*	270*
chemokine (C-X-C motif) ligand 9 (*Cxcl9*)	120	80	80	140	4770*	280*	130	100	160	140	4140*	310*	110
chemokine (C-X-C motif) receptor 3 (*Cxcr3*)	40	30	40	40	30	30	30	30	40	20	30	30	40
Stellate cells													
Collagen, type I , α1 (*Col1a1*)	110	90	470	120	130	190	160	110	250	210	150	350	220
Desmin (*Des*)	50	40	60	50	60	60	40	50	60	50	60	60	60
Liver progenitor cells													
Cytokeratin 19 (*Krt19*)	30	40	50	30	20	40	40	30	30	30	30	30	30
Epithelial cell adhesion molecule (*Epcam*)	80	80	100	70	90	80	90	50	70	90	60	70	90
Sinusoid transporter													
ATP binding cassette subfamily C member 1 [*Abcc1* (*Mrp1*)]	20	30	30	30	30	30	30	40	30	30	30	40	30
ATP binding cassette subfamily C member 3 [*Abcc3* (*Mrp3*)]	110	150	220	100	130	110	70	70	140	80	90	200	90
solute carrier family 10 member 1 [*Slc10a1* (*Ntcp*)]	3650	3620	2880	3170	2850	3490	3370	1090**	3090	2930	740**	3120	3320
solute carrier organic anion transporter family, member 1a1 [*Slc21a1* (*Oatp1*)]	1170	1150	840	830	680	880	850	530**	610	730	380**	770	770
solute carrier organic anion transporter family, member 1a2 [*Slc21a2* (*Oatp2*)]	950	480	520	570	220**	1060	730	140**	820	310	90**	900	320
Bile canaliculus transporter													
ATP binding cassette subfamily C member 2 [*Abcc2* (*Mrp2*)]	1870	1510	1880	2740	1510	2570	2910	1030	1860	2640	760**	2000	2690
ATP binding cassette subfamily B member 11 [*Abcb11* (*Bsep*)]	2190	2260	2030	2190	1610	2260	2450	1630	2310	2290	1470	2260	2480
ATP binding cassette subfamily G member 5 (*Abcg5*)	340	240	260	230	190	290	190	100**	120**	40**	130**	160**	80**
ATP binding cassette subfamily G member 8 (*Abcg8*)	170	100	110	110	70	110	70	50**	50**	30**	70**	60**	40**
ATP binding cassette subfamily B member 1A [*Abcb1a* (*Mdr1a*)]	140	130	140	90	110	140	100	60	130	90	80	170	80
ATP binding cassette subfamily B (MDR/TAP) member 1B [*Abcb1b* (*Mdr1*|*Pgy1*)]	140	30	180	60	60	130	40	820*	280*	120*	160	500*	60
ATP binding cassette subfamily B member 4 [*Abcb4* (*Mdr2*|*Pgy3*)]	670	750	620	560	880	680	650	710	950	580	1030	940	530

* means more than twofold higher signal than control or sham group. ** means less than half the signal than control or sham group.